INTERSTELLAR EXTINCTION IN THE ULTRAVIOLET

Robert C. Bless and Blair D. Savage
University of Wisconsin
Madison, Wisconsin

ABSTRACT

Interstellar extinction curves over the region 3600-1100 Å for 17 stars are presented. The observations were made by the two Wisconsin spectrometers on board the OAO-2 with spectral resolutions of 10 Å and 20 Å. The extinction curves generally show a pronounced maximum at 2175 ± 25 Å, a broad minimum in the region 1800-1350 Å, and finally a rapid rise to the far ultraviolet. Large extinction variations from star to star are found, especially in the far ultraviolet; however, with only two possible exceptions in this sample, the wavelength at the maximum of the extinction bump is essentially constant. These data are combined with visual and infrared observations to display the extinction behavior over a range in wavelength of about a factor of 20. The observations appear to require a multi-component model of the interstellar material.

I. INTRODUCTION

Recent observations of the continua of stars in the spectral region shortward of 3000 Å have shown that the nature of the interstellar extinction curve in the ultraviolet is quite different than had been expected on the basis of observations in the visual region of the spectrum. OAO-2 has observed many stars suitable for extinction determinations; preliminary results were reported by Bless and Savage (1970). In this paper we present additional extinction curves derived from pairs of stars which display the broad range of behavior so far found.

II. INSTRUMENTAL AND OBSERVATIONAL CONSIDERATIONS

The observations reported here were obtained with the two objective grating spectrum scanners in the Wisconsin instrument package on the OAO; one is sensitive over the wavelength range from about 3600-1800 Å, the second over the interval 2000-1050 Å. The effective collecting area of each instrument is 265 cm^2 and the nominal resolution of the long and short wavelength instruments is 20 Å and 10 Å, respectively. To scan the spectrum, the gratings are rotated in increments equal to the instrumental resolution; integration times at each grating position may be 64 or 8 seconds (usually the latter). Both analog and digital readouts of the signal from the photomultiplier detectors are stored in the spacecraft memory and transmitted to the ground on command. For more information concerning the Wisconsin instrumentation and its operation, see Code et al. (1970).

Spectral scans of S Mon and ξ Per over the long wavelength and short wavelength ultraviolet regions are given in Figures 1 and 2, respectively. The scans have not been normalized;

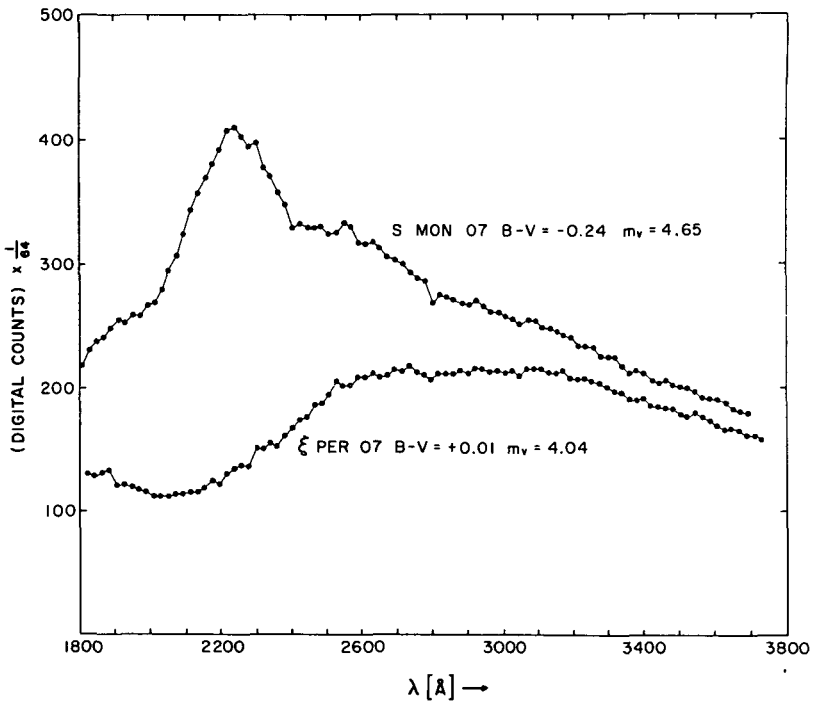

Figure 1.—Spectral scans of S Mon and ξ Per over the region 1800-3700 Å, made by Spectrometer 1 on OAO-2. Note the large extinction effects, especially near 2200 Å. These scans are neither normalized nor corrected for the instrumental sensitivity function.

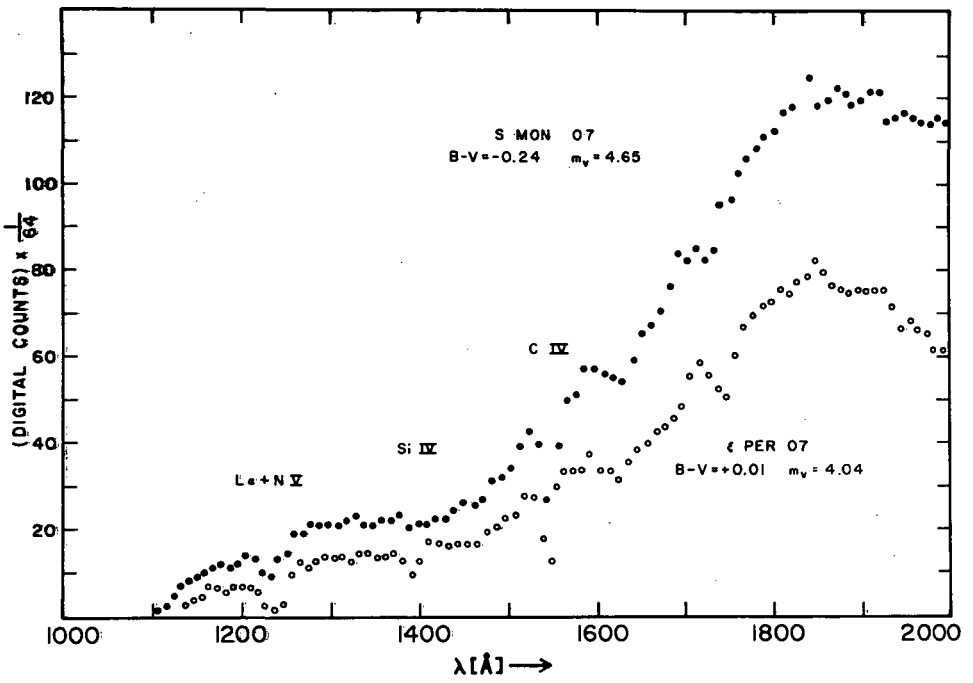

Figure 2.—Spectral scans of S Mon and ξ Per over the region 1100-2000 Å made by Spectrometer 2. As with the curves in Figure 1, these scans are raw data, with only a small, constant background correction made.

note the large extinction effects, especially around 2200 Å, in the reddened star ξ Per. A number of strong lines appear in the spectra of early-type stars shortward of 1800 Å; thus, fitting two scans in this spectral region to a common wavelength scale is straightforward. In the 2000-3000 Å region, however, only the Mg II doublet at 2800 Å appears in the spectra of most early-type stars, and then sometimes only weakly. As a consequence there can be an uncertainty of about ±20 Å in matching two scans over this spectral interval. For our present purposes, however, this uncertainty is of no importance. Sample spectral scans made by these instruments are also given by Code and Bless (1970) as well as in the two papers already mentioned.

The photometric stability of the two scanners is well established. The absolute response of the short wavelength scanner is constant to within 1-2% over a period of many months, whereas the relative response of the longer wavelength instrument is similarly constant. Thus no loss of accuracy whatsoever results in comparing scans made many months apart.

The background count rate of the scanners is primarily due to thermal dark counts, sky light, and scattered light. This background can be determined by observing shortward of the LiF cutoff (1050 Å) of the short wavelength scanner and shortward of the quartz cutoff (1800 Å) of the long wavelength scanner. For early-type stars the background correction is only significant over an interval of a few hundred Angstroms extending longward from 1050 Å; elsewhere the correction is of little consequence.

Since observations of stars made when the OAO is in daylight or traversing the South Atlantic Anomaly of the earth's radiation belt may be affected by extraneous signals and noise, scans which were accidentally made under these circumstances have been rejected.

The field of view of the objective scanners is 8 arc minutes perpendicular to the dispersion and about ±1.5° along the dispersion. Thus, care must be taken to see that stars other than the program star capable of contributing to the ultraviolet flux do not fall within this field. This is routinely checked before an observation is made and, if necessary, the spacecraft is rolled about the scanner optical axis to avoid other stars. In addition, the observations reported here have been checked again; with the exceptions noted in the discussion, only the program stars contribute radiation to the observed flux.

Of obvious importance for ultraviolet extinction determinations is whether or not two stars of the same spectral and luminosity classes and intrinsic visual colors are identical in the ultraviolet. Bless and Savage (1970) gave evidence that such stars do indeed have the same ultraviolet energy distributions; in fact, early B-type stars of the same spectral types and colors, but of any luminosity class II to V, show the same relative flux distribution in the ultraviolet. This characteristic has now been confirmed for many more early-type stars of which a small sample is given in Figure 3, where flux ratios, expressed in magnitudes, are plotted against wavelength. The curves shown were chosen from a series of plots of point-by-point flux ratios made for each pair of stars indicated, each plot in a series for two stars having been shifted slightly in relative wavelength as compared to the next. The particular plots given in Figure 3 were those for which the wavelength scales of the two stars fit best, as indicated by the least scatter of individual points. The longer wavelength scan ratios were then adjusted to fit those over the shorter wavelength region, with the results given in the figure. The sense of the magnitude scale is such that ζ Ori, e.g., is about $0^m.5$ fainter than σ Ori at 1200 Å relative to the V magnitude. Figure 3 also shows that the energy distributions of supergiants is not the same as that of lower luminosity stars of the

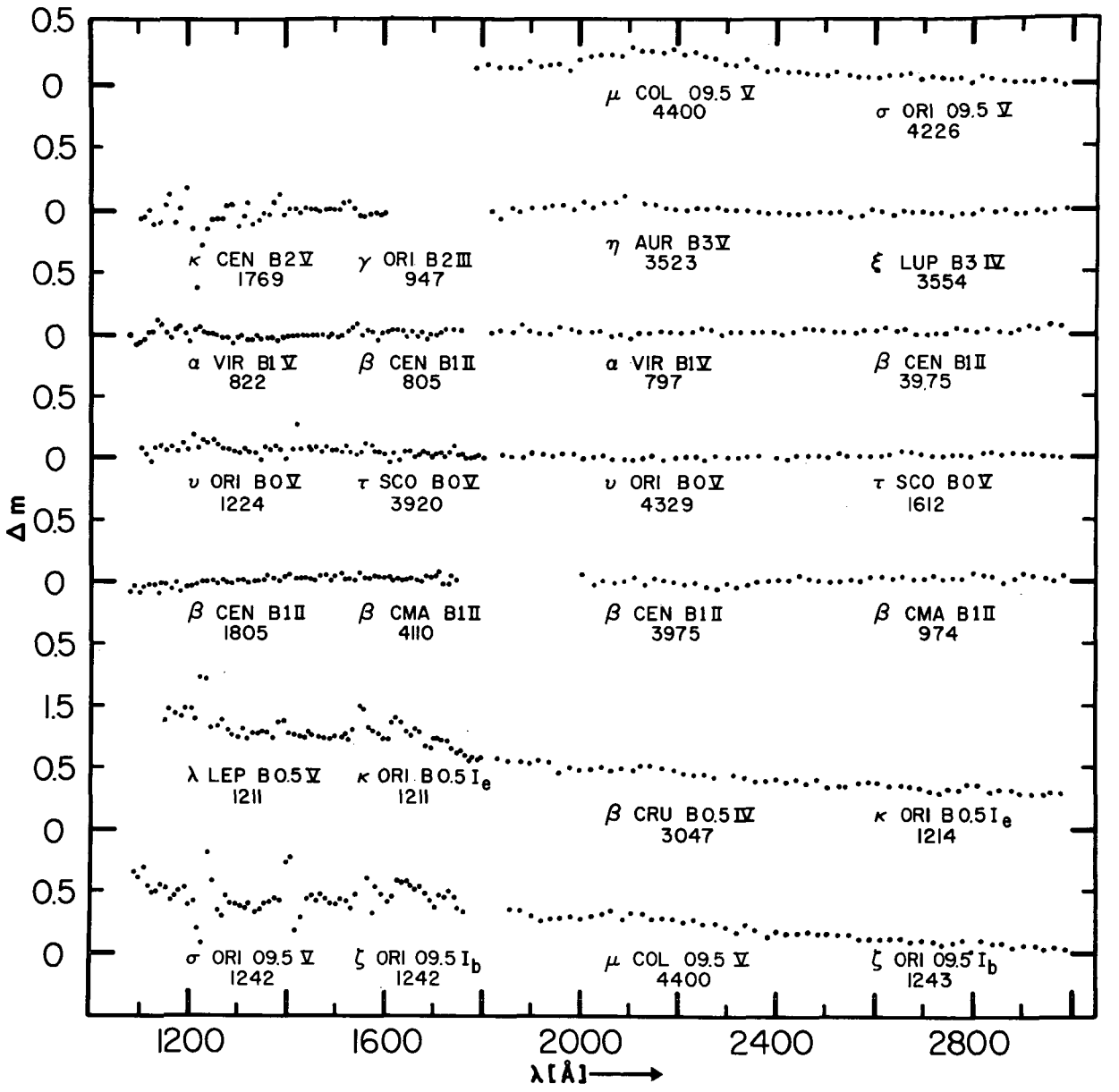

Figure 3.—Ratios, in magnitudes, of ultraviolet energy distributions of little reddened stars of similar spectral types and colors. The data are normalized to the V magnitude and the flux from the star listed on the right of each pair is taken as the numerator in the flux ratio, e.g., F(σ Ori)/F(μ Col). The scatter near Ly α, 1400 Å (Si IV) and 1550 Å (C IV) is caused by differences in these features in the two stars. Note that energy distributions of stars of luminosity classes II to V are essentially identical, whereas supergiants are systematically fainter towards shorter wavelengths as compared with lower luminosity stars.

same spectral type, but that the flux from the former becomes fainter with decreasing wavelength. This effect was first noted by Carruthers (1969) and has been interpreted by Mihalas (1970) as the result of differences in surface gravity and effective temperature between early-type supergiants and dwarfs of the same spectral type. The intercomparison of μ Col and σ Ori in Figure 3 illustrates how ultraviolet energy distributions are modified by only a slight amount of interstellar extinction (σ Ori is $0^m.04$ redder in (B-V) than μ Col).

Calculations have indicated that very rapid rotation should significantly affect the far ultraviolet energy distributions of early-type stars (Collins 1965, Hardorp and Strittmatter 1968). We have looked for such rotation effects by comparing the ultraviolet continua of two stars similar in every way except for their projected rotational velocities. For example, comparison of the energy distributions of δ Lup, α Leo, and ϕ Per ($v \sin i$ = 350 km/sec, 370 km/sec, and 480 km/sec, respectively) with those of a range of stars of similar spectral types and (B-V) colors, but with low rotational velocities, showed no significant differences which could be attributed to rotation. These comparisons were made in the 1050-1800 Å region where the effects are predicted to be greatest. However, we have found that Be stars with strong emission lines in the visual do radiate more energy longward of 2000 Å than do normal stars of the same spectral type. This excess radiation from the Be stars is most likely Balmer continuum emission, similar to that reported by Bohlin (1970) for γ Cas. These same shell stars, however, have normal continua in the spectral region shortward of 2000 Å.

In addition to this fairly detailed search for rotation effects in the continua of a few stars, a cruder search was carried out for about 60 stars with (B-V) color excesses less than $0^m.1$ by plotting their $(1700\text{Å}-V)_o$ colors against their $(B-V)_o$ colors (see Figure 4). To obtain intrinsic colors a small reddening correction was applied using a mean extinction curve (see § IV). As can be seen in the figure, there is no significant difference attributable to rapid rotation, at least at a level important for extinction determinations. The results concerning rotational effects summarized here will be discussed in greater detail in a later paper. For our present purposes we will not use observations in the 2000-3000 Å spectral region of stars which show strong Be characteristics; otherwise we assume that rapid rotation does not significantly distort the continuous spectrum of a star.

Figure 4 also shows that for this sample, unreddened stars of similar intrinsic colors do not differ appreciably in the far ultraviolet; all of the observational points fall within $0^m.25$ of a mean curve. Since the slope of the color-color plot

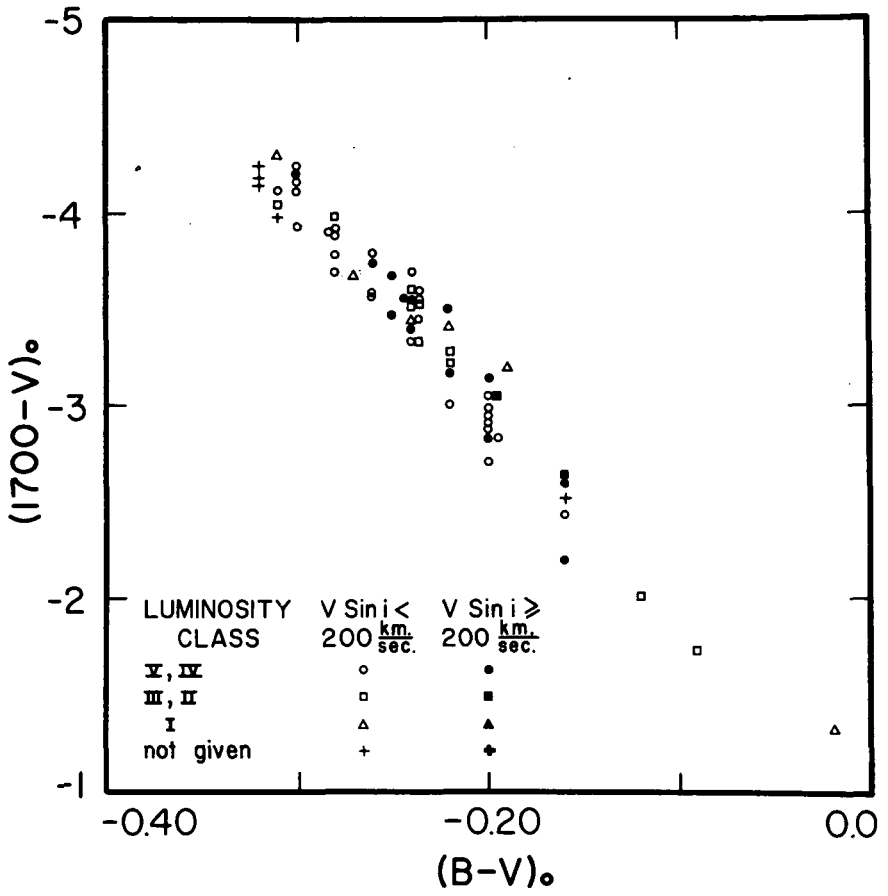

Figure 4.—Color-color diagram for 60 stars with E(B-V) ≤ 0.1, and of a variety of spectral types, luminosity classes, and rotational velocities. Ultraviolet extinction was corrected for by means of the "average" extinction curve shown in Figure 6. No prominent rotational effects are apparent.

of Figure 4 is so large much of the $0^{m}.25$ scatter can probably be explained as small errors in the $(B-V)_o$ determinations. In this diagram, supergiants do not appear systematically fainter in the ultraviolet since their ultraviolet colors are plotted against their visual colors rather than against their spectral types.

In conclusion, the discussion above indicates that one can derive extinction curves by intercomparing reddened and unreddened early-type stars of the same spectral type and of any luminosity class, II through V, or by intercomparing supergiants of the same spectral type. Furthermore, one can intercompare rapidly rotating stars with slowly rotating stars provided Be stars are avoided in the region 2000-3600 Å.

III. THE OBSERVATIONS

Table 1 lists the stars used in this paper for extinction determinations. Wherever possible, photometric data for northern stars were taken from Iriarte et al. (1965) and for southern stars from Cousins and Stoy (1962). Spectral types are those given by Lesh (1968) or by Hiltner, Garrison and Schild (1969) for northern and southern objects, respectively. Intrinsic colors used to form the (B-V) excess are those given by Johnson (1963). Projected rotational velocities (Boyarchuk and Kopylov 1964) are given for stars with v sin i $\geq$ 200 km/sec.

We thought it useful to display all available extinction data for the stars listed in Table 1. For this purpose we used Johnson's (1966) infrared and visual colors for the more heavily reddened star of each pair. Since infrared measurements are not available for several of our comparison stars, we used for the colors of these objects Johnson's (1968) mean values for the appropriate spectral types and luminosity classes. In nearly all of those instances which could be checked, the mean infrared colors well represent the colors of the individual objects.

The procedure by which the infrared, visual and ultraviolet observations were fitted together was straightforward. Differences between the program and comparison stars in their infrared and visual colors were adjusted to $\Delta(B-V) = 1\overset{m}{.}0$ and the V magnitude point set equal to zero. The values so found were plotted as circles in Figures 5a, b, c and d. Flux ratios were formed for the ultraviolet scanner data in the manner previously described for the comparisons of the unreddened stars, and then adjusted to $\Delta(B-V) = 1\overset{m}{.}0$. The longer wavelength data were fitted to Johnson's measurement at 3600 Å ($1/\lambda = 2.78\ \mu^{-1}$) and the shorter wavelength scanner data joined to the longer in the 2000 Å region. Generally, this procedure was satisfactory and only in a few instances was any judgment required to join the scans.

A rather sharp spike appears on some of the curves in Figure 3 and Figures 5a-d, especially near Ly α, but also at 1400 Å (Si IV) and 1550 Å (C IV). This is simply the result of incomplete canceling of the line profile in the two stars in question due either to differences in the profile or to a slight wavelength discrepancy. Such points are not representative of the real observational scatter, which is considerably smaller. It is difficult to make a precise assessment of the errors in these curves, but an estimate can be obtained from the scatter in the curves shown in Figures 3 and 4. Generally the observational error in the longer wavelength region is small, but it increases towards shorter wavelengths pri-

Table 1. Data for Stars Used in Extinction Determination

Star*	V	S. T.	(B-V)	Remarks
ξ Per	4.06	O7.5	+0.01	v sin i = 211 km/sec
15 Mon }	4.66	O7	-0.24	Multiple system; comb. mag. and color; S Mon brightest member
15 Mon }				
ζ Oph	2.57	O9.5 Vnn	+0.02	v sin i = 400 km/sec
μ Col	5.16	O9.5 IV	-0.29	
σ Ori	3.83	O9.5 V	-0.24	Multiple system; composite; mag. and color for A, B, and C
β^1 Sco	2.55	B0.5 V	-0.08	
β Cru }	1.25v	B0.5 III	-0.24	Double, Δm = 10; β CMa variable
β Cru }				
σ Sco	2.89v	B1 III	+0.14	Sp. bin.; primary β CMa type
β Cen	0.60	B1 III	-0.22	Sp. bin.; double
α Vir	0.96	B1 IV	-0.25	Sp. bin.
ρ Oph	4.63	B2 IV/V	+0.22	Multiple system; brightest components B2 and B3; v sin i = 280 km/sec
γ Ori }	1.64	B2 III	-0.21	
γ Ori }				
HD 48099	6.37	O5.5	-0.04	
15 Mon	4.66	O7	-0.24	See ξ Per

Table 1, continued

Star*	V	S. T.	(B-V)	Remarks
19 Cep	5.10	O9.5 Ib	+0.07	Double; $\Delta m = 6$
ζ Ori	1.74	O9.5 Ib	-0.21	Double; O9.5 Ib($2^m.05$) + B3($4^m.2$) comb. mag. and color
HD 47129	6.06	O8f	+0.05	Sp. bin.; companion probably same type; Plaskett's star
λ Ori	3.39	O8	-0.18	Double with Oe5 ($5^m.6$); comb. mag. and color
λ Cep	5.04	O6f	+0.23	
15 Mon	4.66	O7	-0.24	See ξ Per
ζ Per	2.86	B1 Ib	+0.10	Multiple system
β Cen	0.60	B1 III	-0.22	See σ Sco
β CMa	1.98	B1 II/III	-0.24	
$\theta^{1,2}$ Ori	3.98	O8.5	-0.03	Composite color, mag., and s.t.
15 Mon } 15 Mon }	4.66	O7	-0.24	See ξ Per
δ Sco	2.33	B0.5 IV	-0.10	
τ Sco } τ Sco }	2.82	B0 V	-0.25	

Table 1, concluded

Star*	V	S. T.	(B-V)	Remarks
κ Aql	4.95	B0.5 IIIn	0.00	v sin i = 280 km/sec
β Cru	1.25v	B0.5 III	-0.24	See β^1 Sco
χ^2 Ori	4.63	B2 Ia	+0.29	
γ Ori	1.64	B2 III	-0.21	
ω^1 Sco	3.99	B1 V	-0.04	
β Cen	0.60	B1 III	-0.22	See σ Sco
139 Tau	4.83	B1 Ib	-0.07	
β Cen }	0.60	B1 III	-0.22	See σ Sco
β Cen }				
α Cam	4.29	O9.5 Ia	+0.03	
ζ Ori }	1.74	O9.5 Ib	-0.21	See 19 Cep
ζ Ori }				

*The first star of a group is the reddened object; the second and third are the comparison stars observed by Spectrometer 1 and 2, respectively.

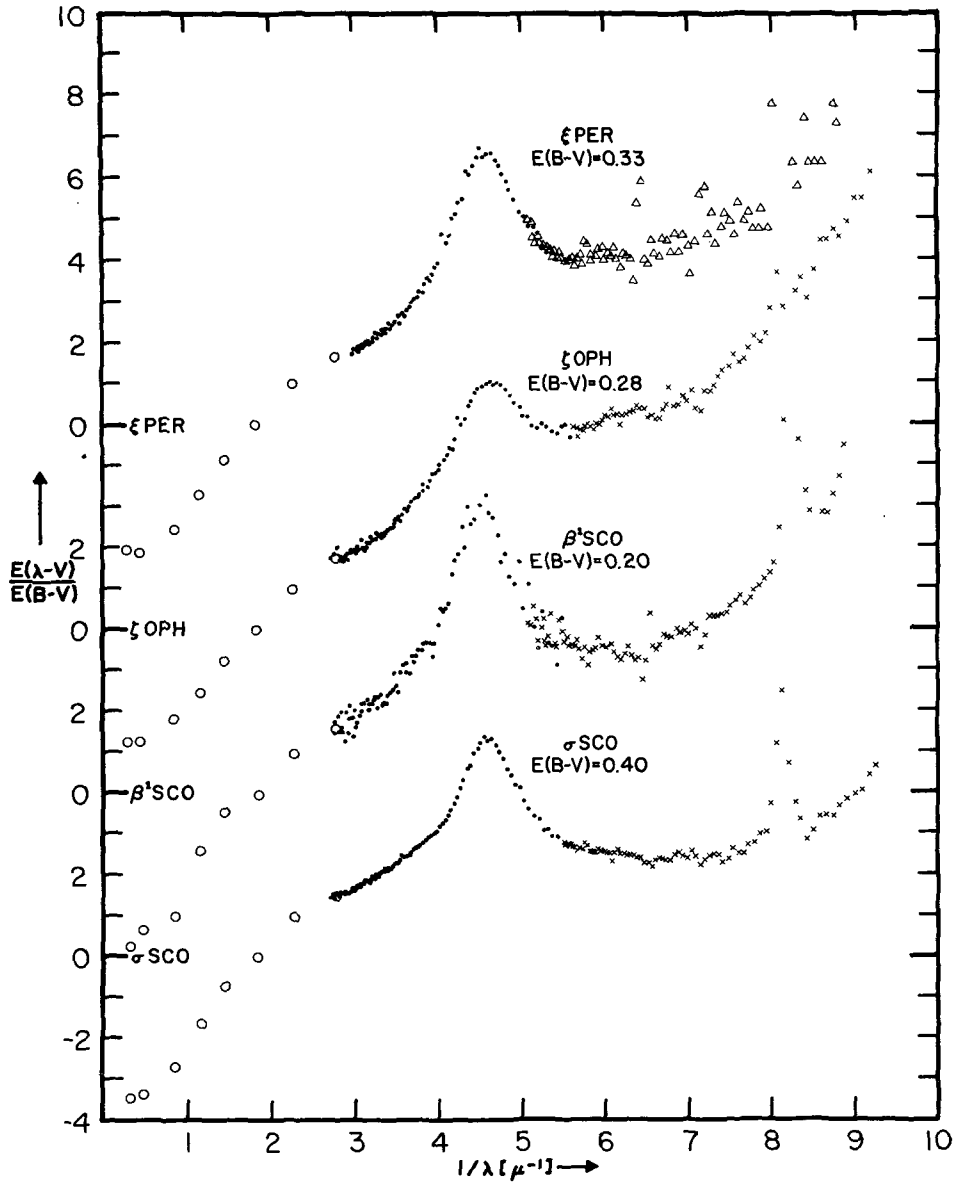

Figures 5a, b, c, d.—Interstellar extinction curves for 17 stars. Data for these stars as well as for the comparison stars are given in Table 1. The dashed lines in the diagrams for 139 Tau, χ^2 Ori, and ζ Per indicate the extinction curve after an approximate correction was applied for the systematically smaller intrinsic ultraviolet flux from a supergiant as compared with that from a lower luminosity star. See the text (§ III) for comments concerning the observational scatter. Extinction curves for β^1 Sco and δ Sco in the 3600-1800 Å region were derived from analog rather than digital data, and are, therefore, of lower quality.

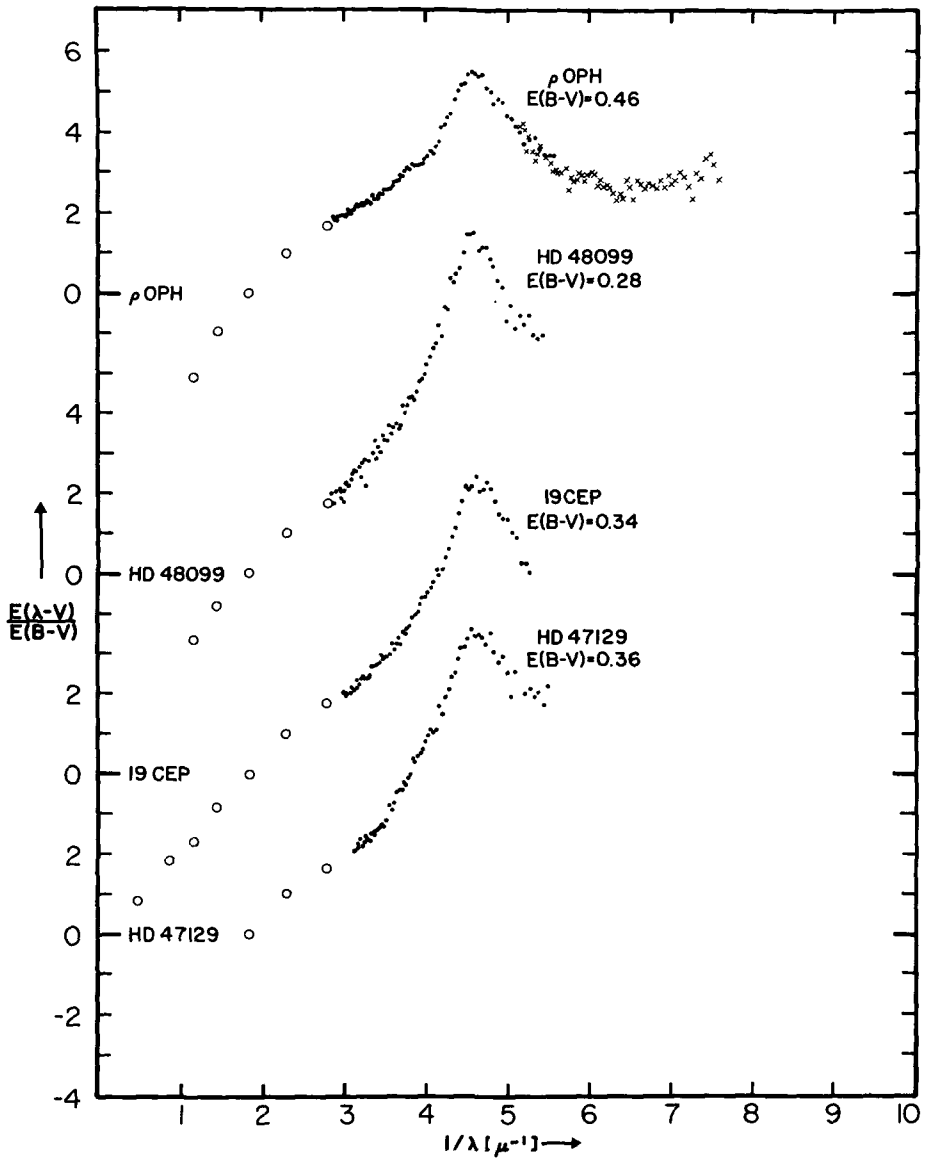

Figure 5b.—See caption for Figure 5a.

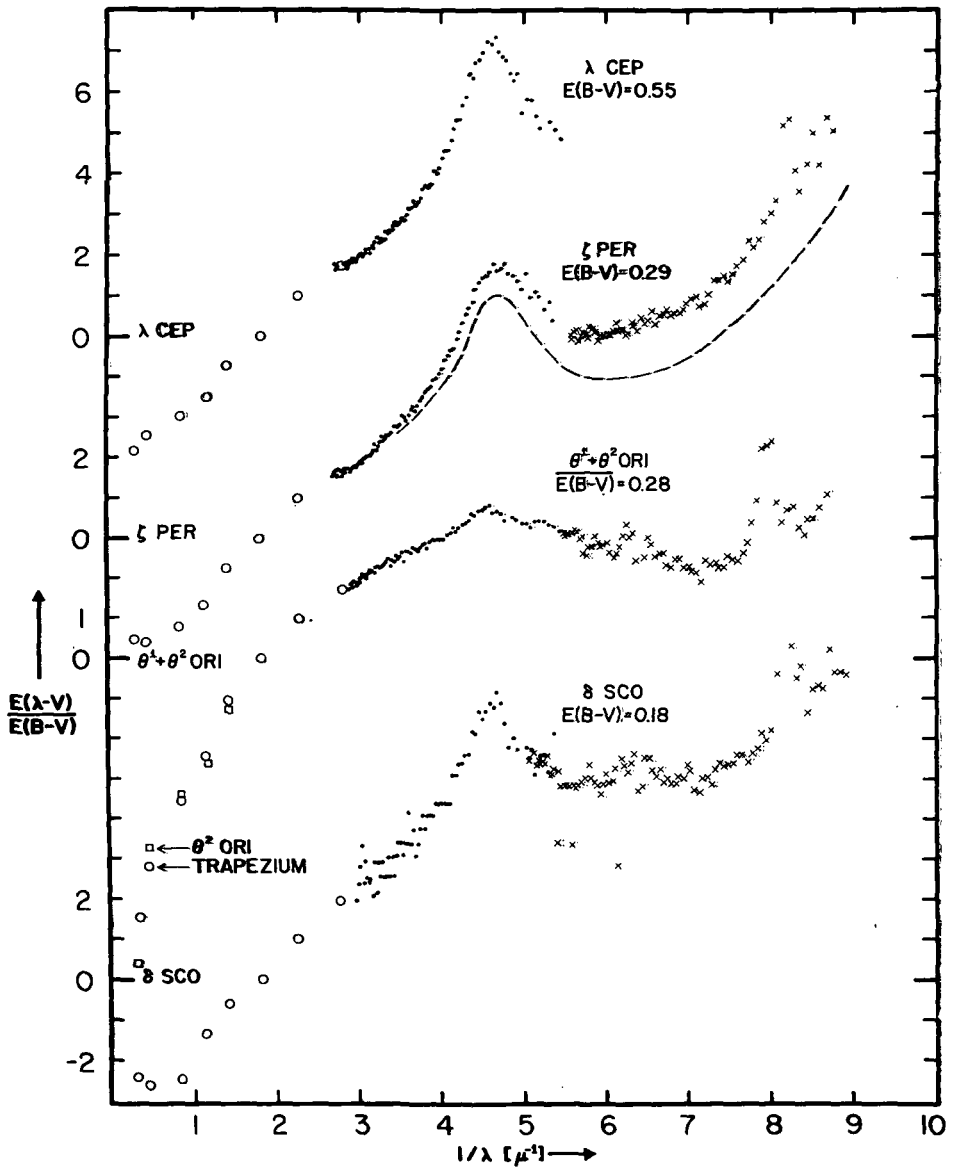

Figure 5c.—See caption for Figure 5a.

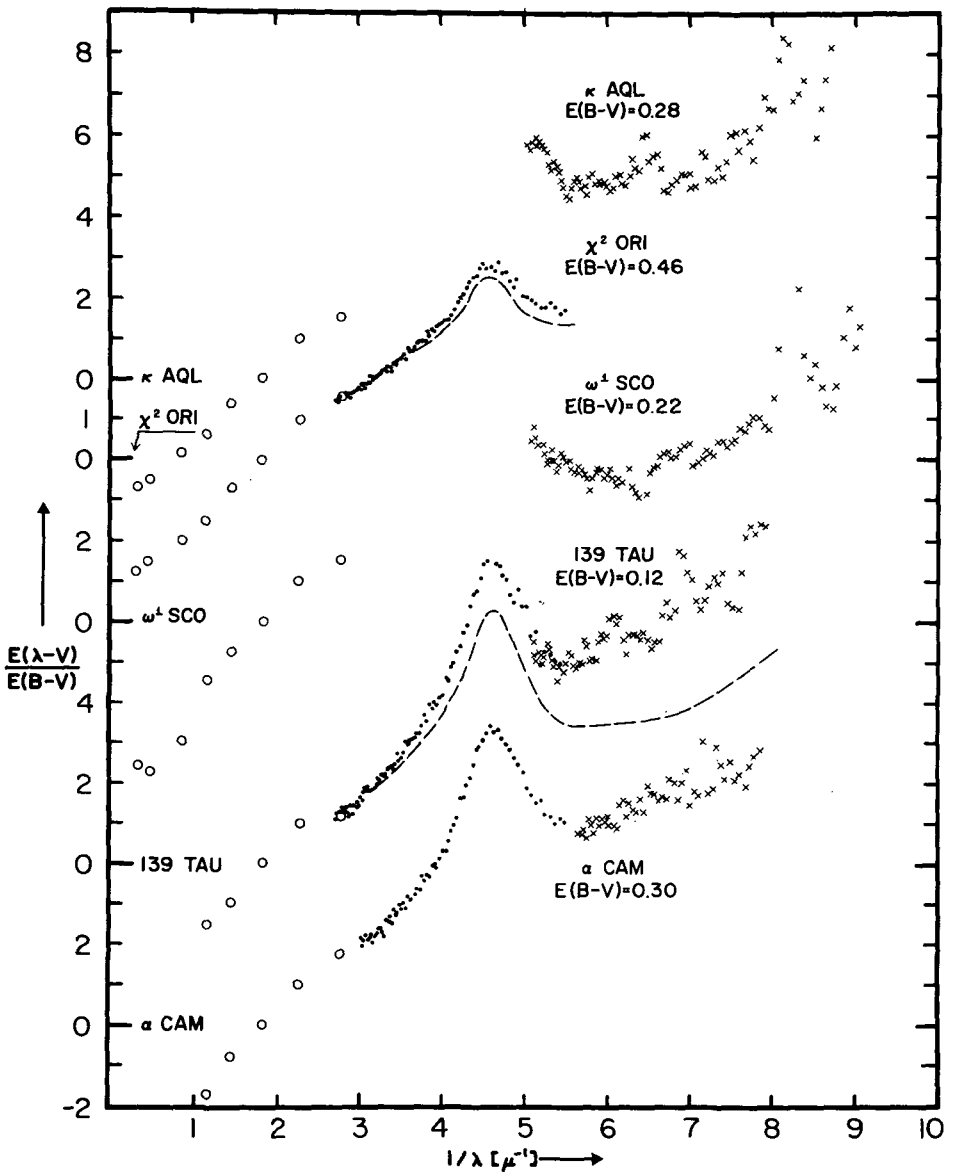

Figure 5d.—See caption for Figure 5a.

marily because of the decrease in instrumental sensitivity. The scatter is not sufficient, however, to mask the overall trend of the points. The precision of the extinction curves depends not only on the accuracy of the ultraviolet observations, but also on that of the (B-V) measurements. Wherever possible, we have used, for a given pair of stars, (B-V) observations made by the same observer in order to minimize systematic errors. For the average Δ(B-V) of the stars used here, about $0^m.30$, a (B-V) error of $0^m.01$ or $0^m.02$ is negligible, but when Δ(B-V) is as small as $0^m.12$ (139 Tau) such an error is significant and the resulting extinction curve uncertain, especially at the shortest wavelengths.

Extinction curves derived from five supergiants are included here. Two of these, α Cam and 19 Cep, were compared with another supergiant, ζ Ori. However, three stars, 139 Tau, χ^2 Ori and ζ Per were compared with less reddened objects of luminosity classes II or III with the consequence that the resulting extinction curves need a slight modification to reflect the previously mentioned intrinsic differences between supergiants and less luminous stars of the same spectral types. A precise correction for the systematic decrease in flux with decreasing wavelength in supergiants as compared to stars of lower luminosity is not possible at this time. A crude correction, however, to the curves for ζ Per, 139 Tau and χ^2 Ori, shown in Figures 5c and d, can be made by decreasing the values of $E(\lambda-V)/E(B-V)$ monotonically so that they are lower at $\lambda^{-1} = 9$ than at $\lambda^{-1} = 3$ by 1.9, 4.0 and 1.2 respectively. These corrections were obtained by applying the observed difference between λ Lep (B0.5 V) and κ Ori (B0.5 Ie) (see Figure 3) to the three supergiants. We have assumed here that the ultraviolet brightness differences for the B1 supergiants (139 Tau and ζ Per) and B2 supergiant (χ^2 Ori) are the same as for B0.5 supergiants.

No serious ambiguities in the data are produced by flux from other stars in the field of view, such stars most often being too faint to contribute more than a few percent to the ultraviolet flux of the program star, or else being of about the same spectral type as the program star, thereby not significantly changing its relative energy distribution.

Generally, the same comments apply in the case of multiplicity of the program or comparison stars themselves. In a few instances, however, lack of information on the nature of the components makes it difficult to determine their effect, so these systems were compared with other objects having, as nearly as possible, identical colors and spectral types. It was found that the colors and spectral types given in Table 1 well represent their ultraviolet spectra. The particularly interesting systems, $\theta^{1,2}$ Ori, σ Sco and ρ Oph will be discussed in the next section.

IV. DISCUSSION

The characteristic features of the ultraviolet extinction curves are: (1) the pronounced bump at about $\lambda^{-1} = 4.6\ \mu^{-1}$; (2) the minimum in extinction which occurs in the region $\lambda^{-1} \simeq 5.5$ to $7.5\ \mu^{-1}$; (3) the rapid rise in extinction in the far ultraviolet; and (4) the large variations in ultraviolet extinction from object to object, these variations being greatest in the far ultraviolet. The extinction bump has been detected in every extinction curve derived thus far (in addition to the curves presented in this paper the bump has been observed in about 30 other slightly or moderately reddened stars). The wavelength of maximum extinction at the bump is rather well defined with nearly all maxima falling at $\lambda^{-1} = 4.6 \pm 0.1\ \mu^{-1}$ (2175 Å ±25); ζ Oph and ζ Per apparently deviate from this behavior with their maxima falling at $\lambda^{-1} = 4.75 \pm 0.1\ \mu^{-1}$ (2105 Å ±25). It has not been established if this difference is due to real differences in the interstellar extinction or rather to peculiarities of the energy distributions of these two stars over the near ultraviolet. (Before it was recognized that continuous Balmer emission significantly modifies the near ultraviolet spectra of early-type emission line stars, extinction curves derived for Be stars also showed peculiar extinction bumps.) The use of various other unreddened comparison stars for the derivation of extinction curves for ζ Oph and ζ Per produced curves nearly identical to those shown in this paper.

Large variations from object to object occur in the ultraviolet extinction curves. These are illustrated in Figure 6 where we have plotted a number of extinction curves which show the range of behavior in the ultraviolet and infrared extinction. The spread in extinction is greatest in the far ultraviolet, although in a few cases the bump is significantly modified ($\theta^{1,2}$ Ori for example). Incidentally, this variation in extinction requires that, as was the case in this paper, comparison stars be little reddened since otherwise one could be comparing two stars having markedly different ultraviolet extinction characteristics, giving a misleading extinction curve.

Table 2 gives an "average" ultraviolet extinction curve we suggest for general use when more detailed information is not available. The values given in the table do not represent the mean through the envelope of extinction curves given in Figure 6. Rather, since the extinction in the direction of $\theta^{1,2}$ Ori, σ Sco and ρ Oph does not appear to occur commonly, the curve given in the table is the average of all stars except these three and represents our estimate of the most likely extinction to be encountered. Obviously, the applicability of this

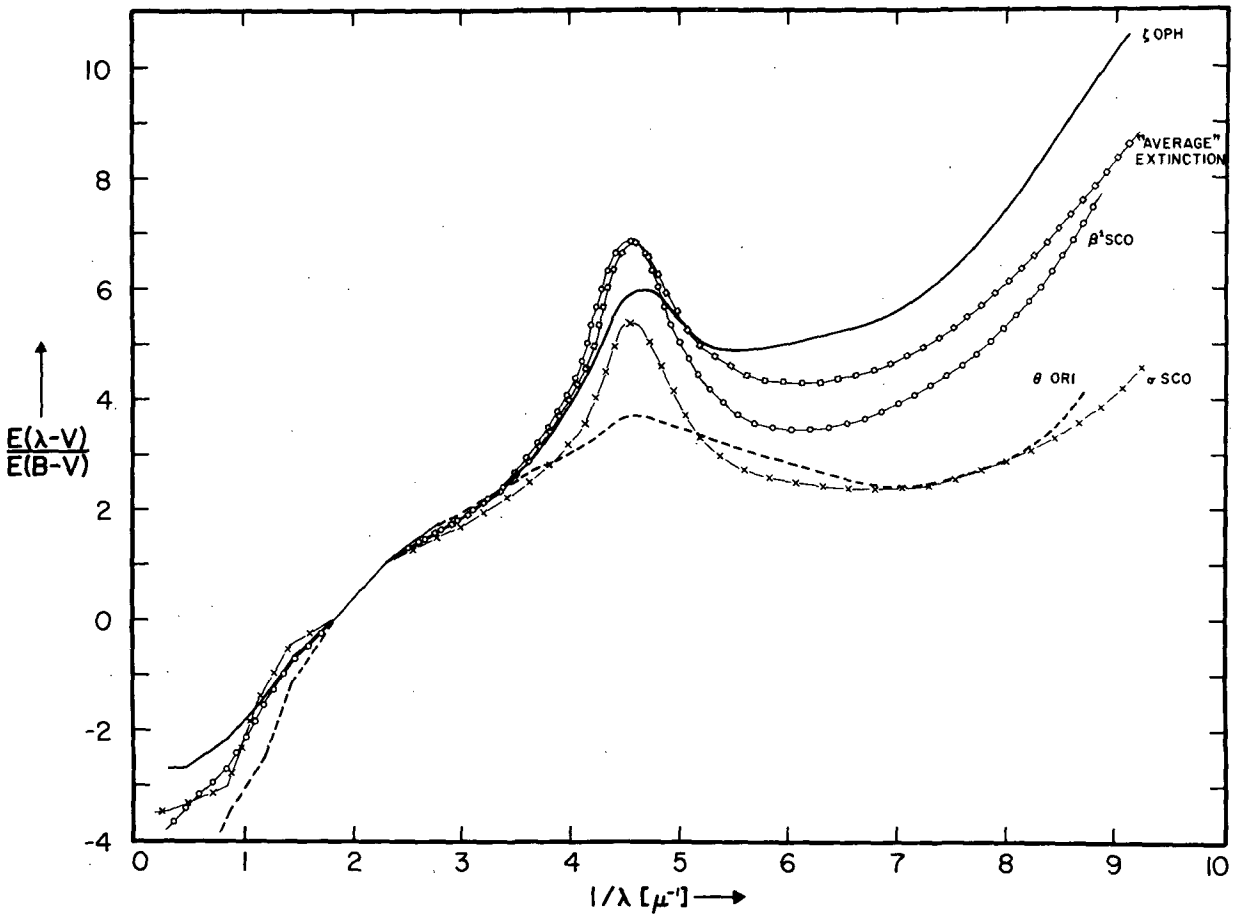

Figure 6.—Interstellar extinction curves which generally define the envelope of all such curves so far obtained. The "average" curve represents the most probable extinction behavior derived from all the extinction data presented in this paper except that for σ Sco, ρ Oph, and $\theta^{1,2}$ Ori.

average curve will depend on the use to which it is put.

The stars $\theta^{1,2}$ Ori, σ Sco and ρ Oph deserve some comment since their extinction curves differ markedly from the majority of those so far found. All three of these stars are multiple: $\theta^{1,2}$ Ori includes six stars ranging from O6 to B3 which have a weighted mean spectral type of O8.6 and a (B-V) color of $-0^{m}.03$, and so a color excess of $+0^{m}.28$. ρ Oph consists of five stars, the brightest two of which are B2 IV and V stars and provide most of the system's radiation; the next brightest, 2 magnitudes fainter, is a B3 star, whereas the faintest two stars contribute little radiation to the system. σ Sco is the simplest of these systems, being the brighter

Table 2. "Average" Ultraviolet Extinction Curve

$\lambda^{-1}(\mu^{-1})$	$E(\lambda-V)/E(B-V)$
3.0	1.9
4.0	4.1
4.6	6.8
5.0	5.6
6.0	4.3
7.0	4.7
8.0	6.0
9.0	8.4

component of a single line spectroscopic binary and having another companion, 7 magnitudes fainter; σ Sco itself is a β CMa star. Though these are complex systems, it seems to us that the composite colors and spectral types taken for these objects represent their ultraviolet flux without error significant for our purposes. In particular, the multiplicity of these objects is not responsible for their peculiar extinction curves. There would seem to be three possible alternatives: the energy distributions of the stars are peculiar; a large amount of flux is scattered into the line of sight by dust grains near the star; the extinction properties of the surrounding medium are abnormal.

The first alternative implies that the extinction suffered by these objects is "normal" and that the observed curves are a consequence of the abnormally large flux radiated by these stars between 2500 and 1100 Å, as compared with normal objects of similar spectral type and color. At $\lambda^{-1} = 4.5$, this additional flux amounts to about $0^m.45$, $0^m.50$, $0^m.75$; at $\lambda^{-1} = 6.0$, $0^m.65$, $0^m.70$ and $0^m.40$; at $\lambda^{-1} = 8.0$, $1^m.0$, $1^m.3$ and $0^m.9$, for ρ Oph, σ Sco and θ Ori, respectively. Now since it is in the ultraviolet that these stars radiate most of their energy, these extra fluxes imply a very large increase in the total energy they emit. Opacity sources for early-type atmospheres would seem to be well understood; it is difficult to see how models based on these sources could successfully predict fluxes in the visual and at the same time be wildly incorrect in the ultraviolet. The contention by Weber et al. (1971) that some unreddened stars are abnormally bright in the ultraviolet should be considered with caution; the relatively low photometric accuracy of their data seems to us to vitiate such a conclusion especially in view of the results on 60 stars presented in Figure 4.

Since all three of these systems are embedded in nebulosity, the possibility exists that associated dust scatters radiation into our line of sight. Such a possibility cannot be ruled out with the data presently available. Simple theoretical calculations of Code (private communication) indicate, however, that under the assumption of spherical geometry and isotropic scattering, grain albedos of nearly one would be required to produce the modifications observed.

The most plausible explanation of these curves seems to us to be that the effect is at least primarily one of anomalous extinction produced by material near the star whose radiation field has modified the grain size distribution and perhaps the composition of the dust. Destruction of the small particles responsible for the far ultraviolet extinction would tend to make the extinction here grey, as is observed. ρ Oph and σ Sco are located in the same association; their extinction curves are similar. In the far ultraviolet they show much the same behavior as $\theta^{1,2}$ Ori, whereas they differ markedly from $\theta^{1,2}$ Ori near the extinction peak. This, along with the anomalous infrared extinction for these three objects, would seem to be more naturally explained by a multi-component model of interstellar grains, such as Gilra (1971) has recently described.

Although the sample of stars is small, we have looked for possible systematic behavior in the variations found in the extinction curves. A convincing systematic effect is that the stars $\theta^{1,2}$ Ori, σ Sco and ρ Oph, all of which have less than normal ultraviolet extinction, also show a large E(V-I)/E(B-V). Apparently, large variations in the ultraviolet extinction are related to variations in the infrared. The characteristics of the extinction bump do not appear to be simply related with infrared extinction. However, one might note that in the two cases where the bump occurs at $\lambda^{-1} = 4.75\ \mu^{-1}$ rather than at $4.6\ \mu^{-1}$, there is also a large far ultraviolet extinction. One possible explanation is that the material responsible for the large far ultraviolet extinction has disturbed the extinction in the region of the bump to such an extent that the bump has been shifted toward shorter wavelengths. If this is the case, however, it is difficult to understand why the star, α Cam, exhibits a "normal" bump and large far ultraviolet extinction. In the data we have presented, there exists a weak inverse correlation between the normalized extinction at the bump and the (B-V) color excess. However, the small sample of stars and the fact that a number of the most highly reddened stars ($\theta^{1,2}$ Ori, ρ Oph and σ Sco) have abnormal ultraviolet and infrared extinction makes this correlation suspect. The position of the far ultraviolet minimum is related to the amount of far ultraviolet extinction in the sense that the

minimum occurs at shorter wavelengths in those cases where the far ultraviolet extinction is smaller.

The extinction curves presented in this paper are not suitable for carrying out a detailed search for possible new diffuse absorptions in the ultraviolet. For many of the curves illustrated in Figures 5a-d there was not a precise spectral match between the two stars which were compared. As a result, many curves contain spurious spikes near the strong stellar ultraviolet lines. However, a reasonably good spectral match was obtained for σ Sco (see Figure 5a). In this case an upper limit to central depths of possible diffuse absorptions as observed with 20 Å and 10 Å slots is found to be approximately 10%. One should compare this upper limit with the observed central depth for the diffuse feature at 4430 Å in σ Sco of 5.7% (Duke 1951). A later paper will be devoted to a much more careful search for possible new diffuse features and for fine structure in the new extinction curves.

The stars studied in this paper are relatively nearby and are therefore unsuitable for investigating any possible dependence of extinction on local galactic structure.

We will not attempt to present a detailed interpretation of the new extinction curves but rather, will review briefly some of the past work to assess its applicability to these results. Much effort has been concerned with attempts to identify the material responsible for the ultraviolet extinction bump and a large number of suggestions have emerged. For example, Stecher (1969), Bless and Savage (1970), Gilra (1971, 1972) and Wickramasinghe and Nandy (1971) believe graphite particles may be responsible for the bump; Huffman and Stapp (1971) attribute the bump to silicates; Manning (1971) suggested quartz, whereas Graham and Duley (1971) indicated that solid hydrocarbons can produce the ultraviolet bump. While it is fair to say that at the present time a conclusive identification of the material responsible for the bump has not been made, the case for graphite seems to be getting stronger. Wickramasinghe and Nandy (1971b) and Gilra (1972) demonstrated that the suggestion of Huffman and Stapp (1971) that silicates are responsible for the 4.6 μ^{-1} feature is unlikely because of the severe size distribution restrictions required to produce a pronounced bump from silicates. A critical review of all the suggestions and a discussion of the physics of extinction bumps is given by Gilra (1972), who concluded that the most likely cause of the extinction bump is plasma oscillations in small (mean radius $\simeq$ 100 Å), nearly spherical, uncoated graphite particles. If the bump is produced by graphite, the particles must be small and nearly spherical in order to produce a relatively narrow bump at the observed position of 4.6 μ^{-1}. As can be seen in the curves of Bless and Savage (1970) and Gilra (1971), large (radius > 200 Å) spherical graphite particles produce

broad bumps which are centered at much longer wavelengths than observed. This is why Bless and Savage (1970) suggested small graphite particles as a possible explanation of the ultraviolet bump. If the graphite particles are small compared to the wavelength, then the position of the bump becomes nearly independent of the details of the size distribution of the particles. This is an important point because most of the observed bumps occur at $\lambda^{-1} = 4.6\ \mu^{-1}$ and it is unreasonable to expect the interstellar particles to have the same size distribution everywhere. Gilra (1972) also points out that the position of the bump is dependent on the particle shape. It was of great interest to us to note that the pronounced ultraviolet extinction bump may not only provide clues on the kind of material producing the extinction but also on the size and shape of the interstellar particles.

There have been various attempts to explain the entire extinction curve. The most complete description is that of Gilra (1971) who attempted to explain all the existing observational data on interstellar grains in terms of a mixture of particles of graphite, silicates, and silicon carbide; these are the three materials Gilman (1969) predicted would form in the atmospheres of cool stars. Gilra was able to reproduce quite well much of the observational data on interstellar grains with his model, but his proposed mixture does contain many variable parameters. The new extinction data presented in this paper strongly suggests that interstellar grains likely have a variety of compositions. The stars σ Sco, β^1 Sco and ξ Per in Figure 5a all have extinction bumps which are quite similar whereas each has a different amount of far ultraviolet extinction. One obvious explanation for this effect is that the constituent responsible for the far ultraviolet extinction is different from that producing the bump. As mentioned earlier, a similar conclusion is reached if one compares the extinction curves for σ Sco and ρ Oph with that for $\theta^{1,2}$ Ori. In this case the far ultraviolet extinction is similar in the three stars while the bump is nearly absent in $\theta^{1,2}$ Ori.

In attempting to interpret these new data one should consider molecules as a possible source of continuous extinction. Stecher and Williams (1969) suggested that photodisassociation of the H_2+ molecule may be partly responsible for the extinction rise in the far ultraviolet. Using the H_2+ photodisassociation cross-sections of Solomon (1964) one finds that for approximately 4.0×10^{17} H_2 + molecules cm^{-2} in the ground vibrational state the extinction at 1150 Å is 3.0 which is about what is observed by OAO in the star ξ Per (see Figure 5a). Furthermore, ξ Per is the star in which Carruthers (1970) detected an H column density of 1.3×10^{20} molecules cm^{-2}. Therefore if 0.3% of the molecular hydrogen in interstellar

clouds is ionized one could understand the rise in far ultraviolet extinction in ξ Per. However, recent radio searches for H_2^+ (Encrenaz and Falgarone 1971; Jefferts et al. 1970) have failed to detect the molecule.

In addition to reducing more data of the kind presented here, future work will be concerned with the behavior of the extinction bump in a large number of stars with a wide range in reddening, in an attempt to better understand this important feature. Also, the OAO filter photometry data will be reduced for extinction purposes. Many of the stars observed photometrically are considerably fainter than those observed spectrophotometrically so that results pertaining to a larger volume of space will become available.

We would like to thank Dr. A. D. Code and Mr. D. P. Gilra for helpful discussions. This work was supported by the National Space and Aeronautics Administration through NAS 5-1348.

REFERENCES

Bless, R. C. and Savage, B. D. 1970, I.A.U. Symp. No. 36, p. 28.
Boyarchuk, A. A. and Kopylov, I. M. 1964, Isz. Krym. Astron. Obs. 31, 44.
Carruthers, G. R. 1969, Ap. and Space Sci. 5, 387.
_____ 1970, Ap. J. (Letters) 161, L81.
Code, A. D. and Bless, R. C. 1970, I.A.U.Symp. No. 36, p. 173.
Code, A. D., Houck, T. E., McNall, J. F., Bless, R. C. and Lillie, C. F. 1970, Ap. J. 161, 377.
Collins, G. W., II 1965, Ap. J. 142, 265.
Cousins, A. W. J. and Stoy, R. H. 1963, Bull. Roy. Obs., No.64.
Encrenaz, P. J. and Falgarone, E. 1971, Ap. Letters 8, 187.
Gilman, R. C. 1969, Ap. J. (Letters), 155, L185.
Gilra, D. P. 1971, Nature 229, 237.
_____ 1972, in preparation.
Graham, W. R. M. and Duley, W. W. 1971, Nature 232, 43.
Hardorp, J. and Strittmatter, P. A. 1968, Ap. J. 151, 1057.
Hiltner, W. A., Garrison, R. F. and Schild, R. E. 1969, Ap. J. 157, 313.
Huffman, D. R. and Stapp, J. L. 1971, Nature 229, 45.
Iriarte, B., Johnson, H. L, Mitchell, R. I. and Wisniewski, W. K. 1965, Sky and Tel. 30, 21.
Jefferts, K. B., Penzias, A. A., Ball, J. A., Dickinson, D. F. and Lilley, A. E. 1970, Ap. J. (Letters), 159, L15.
Johnson, H. L. 1963, Basic Astronomical Data, Ed. K. Aa.Strand (Chicago: University of Chicago Press), p. 204.
_____ 1966, Comm. Lunar and Planet. Lab. 4, 99.

_____ 1968, Nebulae and Interstellar Matter, Ed. B. M. Middlehurst and L. H. Aller, p. 167.
Lesh, J. R. 1968, Ap. J. Suppl. 17, 371.
Manning, P. G. 1971, Nature 229, 115.
Mihalas, D. 1970, Ap. and Space Sci. 8, 50.
Solomon, P. M. 1964, Ph. D. Thesis, University of Wisconsin.
Stecher, T. P. 1969, Ap. J. (Letters), 157, L125.
Stecher, T. P. and Williams, D. A. 1969, Ap. Letters 4, 99.
Weber, S. V., Henry, R. C. and Carruthers, G. R. 1971, Ap. J. 166, 543.
Wickramasinghe, N. C. and Nandy, K. 1971a, Nature, 229, 81.
_____ 1971b, Nature 230, 16.